Proceedings of the 3rd International Conference on Mechanical Engineering and Mechatronics
Prague, Czech Republic, August 14-15, 2014
Paper No. 154

Study on Cable Based Parallel Manipulator Systems for Subsea Applications

Asim Ghaffar, Mahir Hassan*
King Fahd University of Petroleum and Minerals (KFUPM)
Department of Mechanical Engineering
Dhahran, 31261, Saudi Arabia
mahirhassan@kfupm.edu.sa

Abstract **–** In this study, ship position optimization is conducted on a redundant cable-driven parallel manipulator (CPM) operating inside deep sea. The workspace of the manipulator is analysed and ship position optimization has been performed to maximize the workspace and stiffness of the manipulator. The optimization is demonstrated with eight and ten ships CPMs. The workspace and stiffness of the manipulator is improved with more number of cables in a CPM.

Keywords**:** Cable-driven manipulator, Workspace, Wire-driven manipulator, Marine platform, Stiffness.

1. Introduction

Cable based parallel manipulators (CPM) are a type of parallel manipulators that has recently gained interest in large workspace manipulation tasks. Instead of rigid links, cables are used in order to manipulate the moving platform. It has a relatively simple form, with multiple cables attached to the moving platform or the end effector. The manipulator is controlled by cables attached to motors that can extend or retract the cables. These motors may be fixed in a specific location or mounted to moving bases.

A wide variety of cable based parallel manipulators have been developed. Because of the physical characteristics of the cables, workspace design and analysis are different from those of conventional parallel manipulators. There have been a number of CPM designs presented in the literature such as NIST Robocrane (Albus et al., 1993), Falcon-7 (Kawamura et al., 1995), WARP (Maeda et al., 1999), WiRo (Ferraresi et al., 2004) DeltaBot (Behzadipour and Khajepour, 2005), and the hybrid cable-actuated robot developed by Mroz et al (2004). As cables can apply force in one direction only, CPM needs to be redundantly actuated in order to keep all cables in tension at all times during its operation (Hassan and Khajepour, 2009), (Verhoeven and Hiller, 2004), (Gorman et al., 2001). The workspace of the CPM has been studied by many researchers. Several definitions of workspace characterization can be found in the literature (Verhoeven and Hiller, 2000), (Alp and Agrawal, 2002), (Bosscher and Ebert-Uphoff, 2004). A stiffness model for cable based manipulators was developed by Behzadipour and Khajepour (2005). The optimization of the cables tension distribution is also studied by many researchers (Hassan and Khajepour, 2011)

One important application that has not been fully investigated for cable-driven manipulators is in the subsea environment. This study is focused on the workspace and stiffness analysis of the cable driven parallel manipulators operating inside deep sea. The manipulator is capable of 6DOF placed undersea and is connected through redundant cables to the moving ships at the sea surface. Ship position optimization will be conducted so as to maximize the workspace and stiffness of the manipulator. The study will be demonstrated by eight and ten cables CPM.

2. Manipulator Layout

When redundant cables are used to operate a cable-driven parallel manipulator (CPM), multiple solutions exist for the cable tensions given a certain wrench at the end effector. The CPM consists of a rectangular platform attached to the moving ships at the sea surface through cables. The manipulator is operating below the sea surface. The cables with lengths $L_1, L_2, \ldots, L_n$ are attached to the manipulator at one end at points $B_1, B_2, \ldots, B_n$, and to the individual ships on the sea surface at points $A_1 A_2 \ldots . A_n$. This is shown for eight cables CPM in figure 1 and for ten cables CPM in figure 2. The global coordinate frame x-y-z is fixed at the center of the cylindrical workspace at a depth of $h = 50m$ below the sea surface with its axes aligned with the sides of the moving platform. The moving coordinate frame $x_p y_p z_p$ is attached at the center P of the manipulator with its axes aligned with platform dimensions m, n and o. The platform dimensions are given as $m = 4m$, $n = 5m$ and $o = 0.3m$. The moving platform can translate as well as rotate by extending or retracting the cables or by moving the ships along x-y-z axis. Each ship can move in a circular trajectory of radius 50m. The ship positions will be optimized along this circular trajectory so that the manipulator can have maximum workspace and stiffness.

The moving platform will be equipped with grippers to perform pick and place operations and to perform transportation of objects from one place to another under the sea surface. The positions of the ships will be optimized utilizing cable tension minimization scheme developed by Dykstra (1983) and applied by Hassan and Khajepour (2011) in cable manipulators.

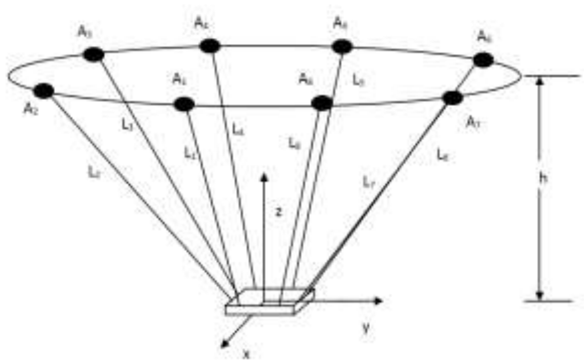

Fig 1. A schematic of the CPM with eight cables.

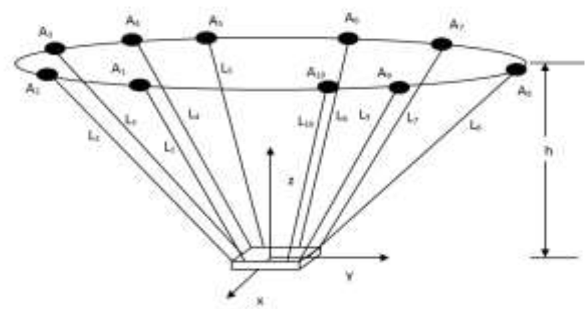

Fig 2. A schematic of the CPM with eight cables.

3. Static Analysis: Bounded Cable Tensions

When a task is performed by the manipulator, the end effector exerts force and moment on the external environment. As the manipulator is operating inside deep sea, various sea forces are acting on the platform. In this study, only the weight of the manipulator and the buoyancy force is considered and the dynamic forces are neglected. Because, it is assumed that the manipulator will be moving at a very low velocity such that the dynamic forces can be neglected.

Static force analysis will be performed in order to determine the feasible workspace of the manipulator. In parallel manipulators, the actuator input wrenches are related to the end-effector output wrench by the transpose of the manipulator Jacobian matrix (Tsai, 1999). Therefore, the equation can be formulated as:

$$\mathbf{w} = \begin{bmatrix} \mathrm{f} \\ \mathrm{m} \end{bmatrix} = -\mathbf{A}\boldsymbol{\tau} \tag{1}$$

Where

$$\mathbf{A} = \begin{bmatrix} \hat{\mathbf{l}}_1 & \cdots & \hat{\mathbf{l}}_i & \cdots & \hat{\mathbf{l}}_n \\ (\mathbf{r}_1 \times \hat{\mathbf{l}}_1) & \cdots & (\mathbf{r}_i \times \hat{\mathbf{l}}_i) & \cdots & (\mathbf{r}_n \times \hat{\mathbf{l}}_n) \end{bmatrix}$$

And $\boldsymbol{\tau}_i > 0\ \forall i$

Here **f** and **m** are the external force and moment applied to the moving platform. 'n' are the number of cables; $\boldsymbol{\tau}$ is an n-dimensional vector of cable tensions; τ_i is the value of tension in the ith cable. $\hat{\mathbf{I}}_i$ is a unit vector in the direction of the force applied by the ith cable and $\mathbf{r}_i$ is the position of the ith cable connection point on the moving platform with respect to its center.

Eq. (1) can be written as:

$$\boldsymbol{\tau} = -\mathbf{A}^{+}\mathbf{w} \tag{2}$$

Where $\mathbf{A}^{+}$ is the Pseudo inverse of matrix **A**, since matrix A is not a square matrix, therefore, it is not invertible. So pseudo-inverse $\mathbf{A}^{+}$ will be taken which is the generalization of the inverse of matrix A. It is used to find the minimum (Euclidean) norm solution to a system of linear equations with multiple solutions. In order to minimize the cable tensions, Dykstra's algorithm will be used. It is an iterative algorithm that can be used to find the minimum-Euclidean-distance projection of a point onto the intersection of a number of convex sets, provided that there intersection is a non-empty set Dykstra (1983). The sequences initiate at the origin and proceed by making successive projections of a point 't' in each iteration. Let A and G be two non-empty convex sets, all sequences will converge to a single point onto G as $i \rightarrow \infty$ which is the minimum Euclidean distance from the initial point. Projection of point 't' on set A is calculated as:

$$proj_A(\mathbf{t}) = (\mathbf{I} - \mathbf{A}^{+}\mathbf{A})\mathbf{t} - \mathbf{A}^{+}\mathbf{w} \tag{3}$$

In Eq. (3), **t** is projected onto the null space of matrix **A** and the result is translated by $-\mathbf{A}^{+}\mathbf{w}$. Similarly, $proj_G(\mathbf{t})$ can be calculated as:

$$proj_G(\mathbf{t}) = [\bar{t}_1 \dots \bar{t}_n]^T$$
$$\bar{t}_i = \begin{Bmatrix} \tau_{i\,min} & t_i \le \tau_{i\,min} \\ t_i & \tau_{i\,min} \le t_i \le \infty \\ \tau_{i\,max} & t_i \ge \infty \end{Bmatrix} \tag{4}$$

Eq. (4) therefore trims all coordinates of 't' that are outside the bounds of the orthant G.

4. Workspace Analysis

The workspace of a cable-driven manipulator is the set of all poses that can be reached such that:

- The tensions in the cables are positive i.e. $\boldsymbol{\tau}_i > 0\ \forall\ i$
- The end-effector should avoid any singular condition i.e. $Rank\ (\mathbf{A}) = n$. This is to make sure that the singularity condition is avoided.

5. Ship Position Optimization to Maximize the Workspace

The inverse kinematics for the proposed design is conducted by applying formulations in Eq. (2). By considering the configuration, a numerical algorithm is being implemented and results have been obtained. For determining the optimum ship positions, brute force search method is utilized. The flow chart of this algorithm is shown in figure 3. For every set of ship positions, it computes the workspace of the manipulator by verifying if the manipulator satisfies the imposed geometrical constraints, tensions in the cables are positive and the manipulator is not at a singular configuration. If the conditions are satisfied, it adds the pose of the manipulator to the workspace. In order to determine the complete workspace, the algorithm repeats the same procedure at all poses of the manipulator. Finally, the above procedure is repeated for all combinations of the ship positions and the positions having maximum workspace are determined.

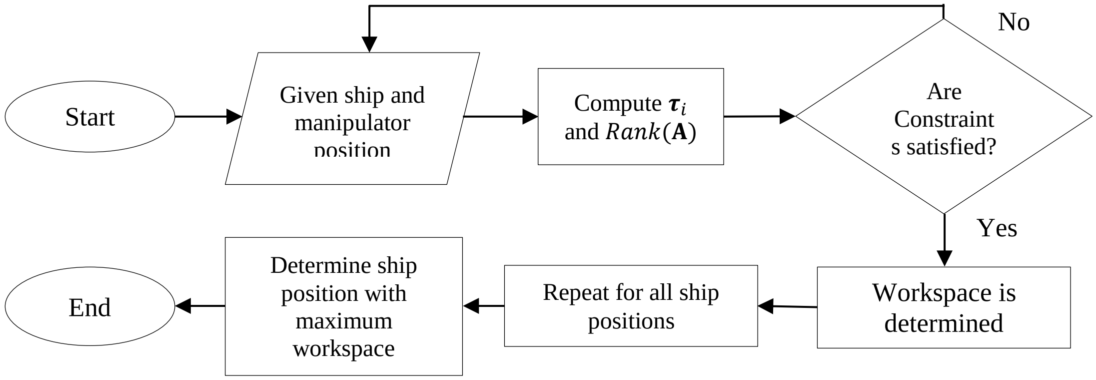

Fig. 3. Algorithm to compute optimum ship positions based on maximizing workspace.

The ship positions obtained from the proposed algorithm are shown in figure 4. With these layouts of the CPM ship positions, the manipulator will have maximum workspace. It is depicted for eight ships in figure 4(a) and for ten ships in figure 4(b).

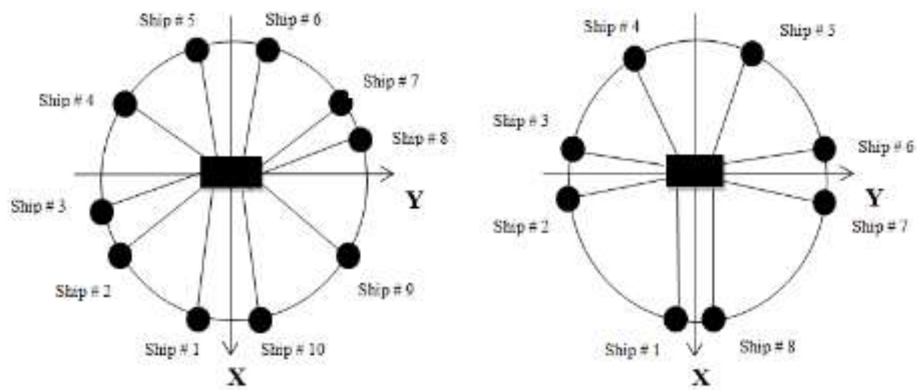

(a) (b)

Fig. 4. Optimized ship positions to maximize workspace (a) for eight ships (b) for ten ships.

Considering the position of the ships in figure 4(a), the results of the numerical analysis are being reported in order to establish poses reachable by the manipulator by considering the given constraints. The position of the manipulator is determined by varying the values of the orientation anglesθ_x θ_y θ_z. The range of values for angle θ_x θ_y θ_z are assumed as [0, 50], [0, 40], [0, 30] respectively. By considering the values of θ_x, θ_y and θ_z the poses of the manipulator obtained are shown in figure 5, 6 and 7 respectively.

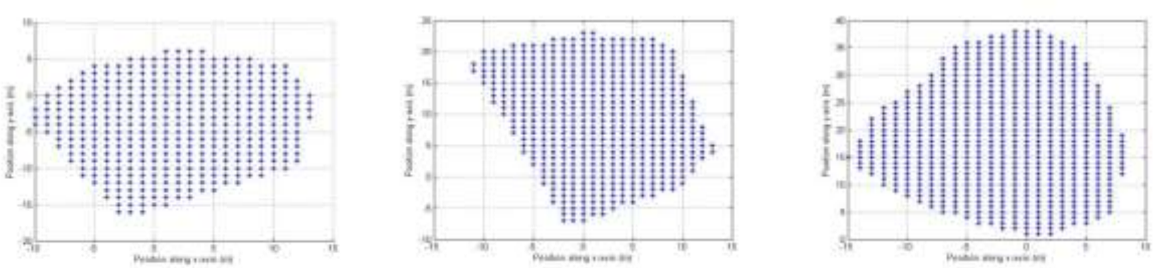

$\theta_x = 0$ $\theta_x = 20$ $\theta_x = 50$

Fig. 5. Manipulators planer workspace x-y by varying angular orientation θ_x with $\theta_y = \theta_z = 0$.

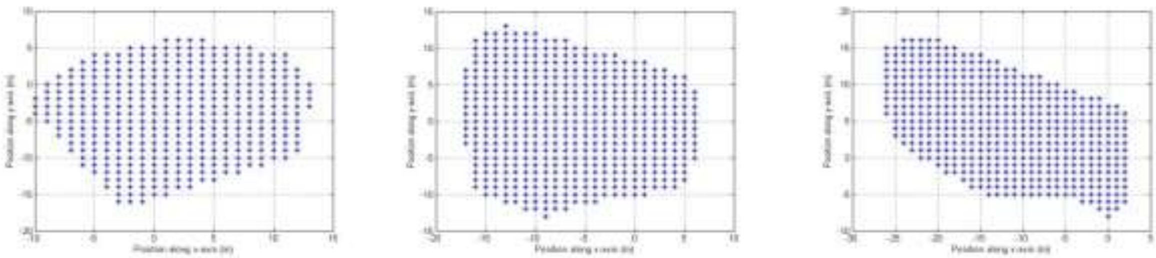

$\theta_y = 0$ $\theta_y = 20$ $\theta_y = 40$

Fig. 6. Manipulators planer workspace x-y by varying angular orientation θ_y with $\theta_x = \theta_z = 0$.

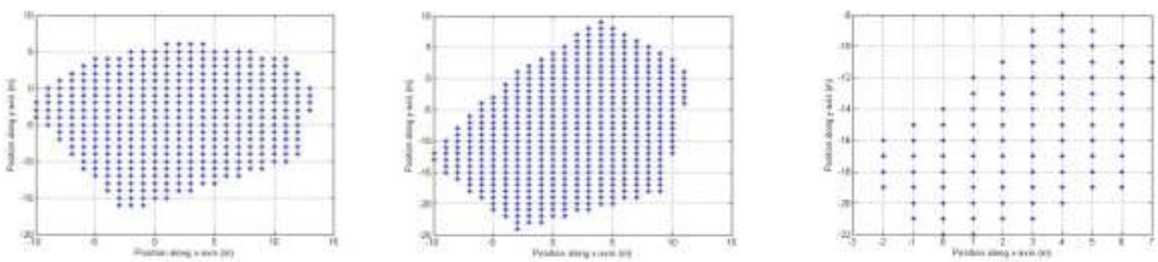

$\theta_z = 0$ $\theta_z = 10$ $\theta_z = 30$

Fig. 7. Manipulators planer workspace x-y by varying angular orientation θ_z and $\theta_x = \theta_y = 0$.

The planer workspace shown in figures 5, 6 and 7 at different orientation values of θ_x, θ_y and θ_z respectively shows a slight increase in the workspace as the orientation angles are increased from zero up to a certain value. But as the manipulator's angle is increased further workspace starts to decrease until it becomes zero. Thus, at very large orientation values, there is a decrease in the workspace of the manipulator. Cable-driven manipulators generally allow limited rotations in their workspace.

6. Ship Position Optimization to Maximize the Stiffness of the Manipulator

In this section, stiffness of the manipulator will be discussed and ship position optimization is performed to maximize the stiffness of the moving platform. The manipulator stiffness depends upon several parameters including material, links dimensions, transmission system, actuation system etc. Based on the work of Behzadipour and Khajepour (2006), the stiffness of the cable based manipulator will be determined. It should be noted that the stiffness of cable driven manipulators is dependent not only on the cable stiffness but also on the cable forces.

In order to determine the optimum positions of the ships, the maximum value of the lower stiffness value is to be calculated. However, translational and rotational stiffness values cannot be compared because they have different physical units. Instead natural frequencies are used because they have common physical units and are indicative of the stiffness matrix. The formula to calculate the natural frequency of the system considering cables as springs is given by:

$$f_j^k = \frac{\sqrt{eig_j(M^{-1}K^k)}}{2\pi} \tag{5}$$

where f_j^k is the jth natural frequency calculated at kth pose. eig_j is the jth eigen value of the stiffness matrix. K^k is the stiffness value of the moving platform at kth pose. **M** is the inertia matrix

The value of f_j^k depends upon the pose of the manipulator and therefore the entire workspace is to be considered when investigating the natural frequency of the manipulator. As mentioned before, in order to find the optimum ship positions, sum of the minimum natural frequencies is calculated for all poses of the manipulator at a particular set of positions of the ships. The function showing the summation of the natural frequencies is expressed as:

$$Sum\ of\ f_{min} = \sum_{j=1}^{n} min_j\left(f_j^k\right) \tag{6}$$

Where $min_j\left(f_j^k\right)$ is the smallest natural frequency at the kth pose of the manipulator. Usually, higher values of natural frequencies imply higher stiffness value. Therefore, in order to maximize the manipulator stiffness, sum of the lowest natural frequency should be maximized. The brute force search method is utilized again to determine the optimum ship positions. The flow chart of the algorithm is shown in figure 8. So, at each set of ship position, sum of f_{min} is calculated for all poses of the manipulator. The position of the ships where sum of f_{min} is maximum would be the optimum position of the ships. The algorithm is studied on CPM with eight and ten ships.

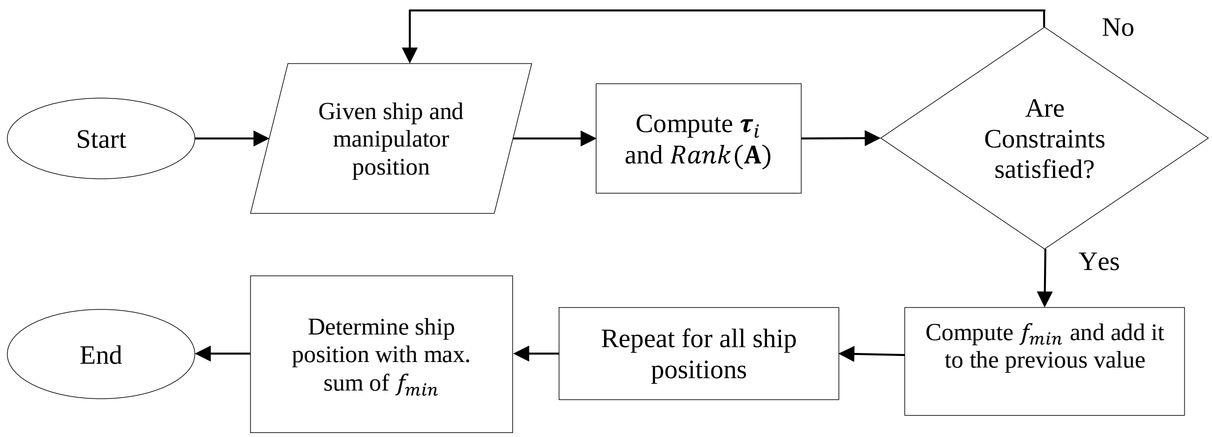

Fig. 8. Algorithm to compute optimum ship positions based on maximizing stiffness.

Results are depicted in figure 9. It shows the layouts of CPM ship positions based on maximizing stiffness and natural frequency of the manipulator. Figure 9(a) & (b) demonstrates the optimum ship positions for eight and ten ships CPM respectively.

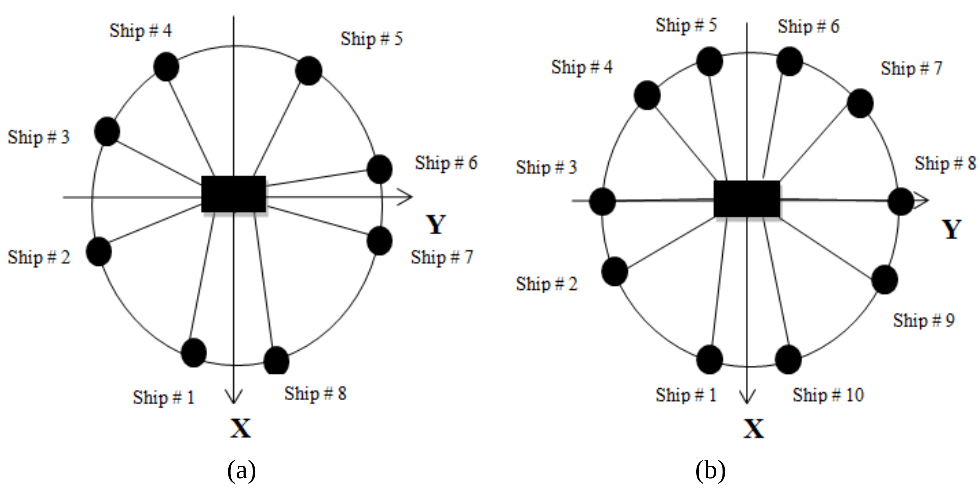

Fig. 9. Optimized ship positions to maximize stiffness (a) for eight ships (b) for ten ships.

Results from the optimization of ship positions based on the workspace and stiffness analysis are summarized in figure 10. It shows the workspace points and sum of the minimum natural frequency obtained for both maximum workspace and maximum stiffness ship positions. By analysing figure 10(a) and (b), it is observed that the workspace with ten cables CPM is greater as compared to eight cables CPM. This is because with greater number of cables, each cable will support a fraction of the applied load at the manipulator, resulting in a better tension distribution among the cables and therefore less chance of having negative cable tensions. Stiffness and natural frequency also follows a similar trend, i.e. the sum of natural frequencies is obtained higher with ten ships as compared with eight ships CPM. This is due to the reason that all cables act like a spring and when more number of springs are connected in parallel, stiffness is found higher. When comparison is observed for the two layouts of CPM, i.e. one that gives maximum workspace and the other that gives maximum stiffness, there obtained a decrease in the stiffness of the manipulator with the layout of CPM giving maximum workspace. Similarly, a decrease in the workspace is reported in CPM with ship positions for maximum natural frequency. This trend is observed in both eight and ten ships CPM.

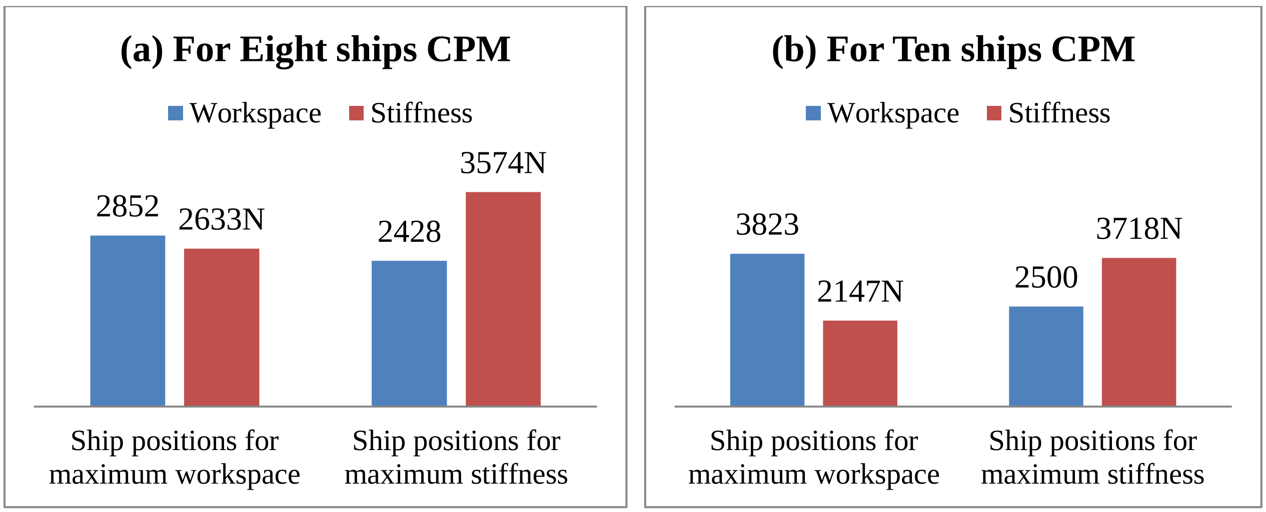

Fig. 10. Comparison of the CPM layouts (a) with eight ships (b) with ten ships.

7. Conclusion

In this study, ship position optimization has been conducted on cable driven manipulators with redundant cables used in subsea applications. The optimization was studied on CPM with eight and ten ships. The workspace and its dependency on the orientation of the manipulator have been analysed. Ship position optimization has been performed to enhance the manipulator's workspace and stiffness. It was observed that the workspace and stiffness was increased with ten ships as compared to eight ships CPM. The performance of the CPM was clearly improved with more number of cables.

Acknowledgements

The author(s) would like to acknowledge the support provided by King Abdulaziz City for Science and Technology (KACST) through the Science & Technology Unit at King Fahd University of Petroleum & Minerals (KFUPM) for funding this work through project No. 11-ELE1623-04 as part of the National Science, Technology and Innovation Plan.

References

Albus J., Bostelman R., Dagalakis N. (1993). The Nist Robocrane, J. Robotic Systems, vol. 10, n. 5,709-724.

Alp A. B., Agrawal S. K. (2002). Cable Suspended Robots: Design, Planning and Control”. Proceedings of the 2002 IEEE International Conference on Robotics and Automation (ICRA), Washington D.C., pp. 4275.4280.

Behzadipour S., Khajepour A. (2005). A New Cable-based Parallel Robot with Three Degrees of Freedom, *Multibody System Dynamics*, vol. 13, pp. 371-383.

Behzadipour S., Khajepour A. (2006) Stiffness of Cable-based Parallel Manipulators with Application to Stability Analysis”, Journal of Mechanical Design, Vol. 128 / 303.

Bosscher P., Ebert-Uphoff I. (2004) “Wrench Based Analysis of Cable Driven Robots”, Proceedings of the 2004 IEEE International Conference on Robotics and Automation (ICRA), New Orelans, pp.834-841.

Dykstra R. L. (1983) An Algorithm for Restricted Least Squares Regression,” J. Amer. Statistical Assoc., vol. 78, pp. 837-842.

Ferraresi C, Paoloni M., Pescarmona F. (2004). A new 6-dof Parallel Robotic Structure Actuated by Wires: The Wiro-6.3, *J. of Robotic Systems*, vol. 21, no. 11, pp. 581-595.

Gorman J. J., Jablokow K. W., Cannon D. J. (2001) “The cable array robot: Theory and experiment,” in *Proc. IEEE ICRA*, Seoul, Korea,pp. 2804–2810.

Hassan M., Khajepour A. (2009) Analysis of a Large-Workspace Cable-Actuated Manipulator for Warehousing Applications”, ASME IDETC/CIE Conference, San Diego, California, USA.

Hassan M Khajepour (2011) A., “Analysis of Bounded Cable Tensions in Cable-actuated Manipulators”, *IEEE Transactions on Robotics*, vol. 27, no. 5, pp. 891-900.

Kawamura S., Choe W., Tanak S. (1995), Development of an Ultrahigh Speed Robot Falcon Using Wire Driven Systems, *Proc. IEEE Int. Conf. on Robot. Autom.*, 215-220.

Maeda K., Tadokoro S., Takamori T., Hiller M., Verhoeven R (1999). On Design of a Redundant Wire-driven Parallel Robot WARP Manipulator in *Proc. IEEE Int. Conf. on Robot. Autom.*, vol. 2, pp. 895-900.

Mroz G, Notash., L. (2004) Wire-actuated Robots with a Constraining Linkage, *J. Robotic Systems*, vol. 21, no. 12, pp. 677-678.

Tsai L. W. (1999) “Robot Analysis-The Mechanics of Serial and Parallel Manipulators”, Wiley-interscience.

Verhofen R. (2004) Analysis of the Workspace of Tendon-Based Stewart Platforms”, Ph. D. thesis, University of Duisburg-Essen.

Verhoeven R., Hiller M.(2000) “Estimating the controllable workspace of tendon-based Stewart platforms,” in *Proc. ARK 7th Int. Symp. Adv. Robot Kinematics*, Protoroz, Slovenia, pp. 277–284.